

servation of the 1:2 complex in the single-jet, but not the twin-jet, experiment gives strong evidence of gas-phase 1:1 complexation. While a 1:2 complex was detected with NH_3 , the corresponding 1:2 complexes with the methylamines were not observed, even under conditions which strongly favor the formation of larger aggregates. Consequently, one may conclude that these adducts are not stable, except for $\text{SO}_2 \cdot 2\text{NH}_3$, even at cryogenic temperatures.

Conclusions

The twin-jet deposition of SO_2 with NH_3 or any of the methylamines gave rise to a 1:1 adduct isolated in argon and nitrogen matrices. The use of single-jet deposition enhanced the yield of complex for most systems, but, in the case of CH_3NH_2 , a dehydration reaction was instead detected. Only for the SO_2/NH_3 system was the 1:2 adduct observed, and this was obtained in best

yield with considerable excess of NH_3 . These adducts were characterized by vibrations of the perturbed SO_2 subunit in the complex; in general the S-O stretching modes shifted to lower energy, while the bending mode shifted to slightly higher energies. These shifts were rationalized in terms of π^* acceptor properties of SO_2 , and increasing donor ability of the methylamines with increasing number of ethyl groups.

Acknowledgment. The authors gratefully acknowledge support of this research by the National Science Foundation, Grant CHE8100119. B.S.A. also thanks the Dreyfus Foundation for a Teacher-Scholar Grant.

Registry No. $\text{SO}_2 \cdot \text{NH}_3$, 29307-29-7; $\text{SO}_2 \cdot 2\text{NH}_3$, 29307-30-0; $\text{SO}_2 \cdot \text{C}_2\text{H}_5\text{NH}_2$, 67592-19-2; $\text{SO}_2 \cdot (\text{CH}_3)_2\text{NH}$, 21326-49-8; $\text{SO}_2 \cdot (\text{CH}_3)_3\text{N}$, 17634-55-8; SO_2 , 7446-09-5; NH_3 , 7664-41-7; CH_3NH_2 , 74-89-5; $(\text{C}_2\text{H}_5)_2\text{NH}$, 124-40-3; $(\text{CH}_3)_3\text{N}$, 75-50-3.

Matrix Isolation Infrared Spectra of Dioxygen Adducts of Iron(II) Porphyrins and Related Compounds

T. Watanabe, T. Ama, and K. Nakamoto*

Todd Wehr Chemistry Building, Marquette University, Milwaukee, Wisconsin 53233 (Received: May 2, 1983; In Final Form: June 16, 1983)

The O_2 stretching bands of the following dioxygen adducts were located in Ar matrices at ~ 15 K: $\text{Fe}(\text{TPP})\text{O}_2$ (1195 and 1106 cm^{-1}), $\text{Fe}(\text{OEP})\text{O}_2$ (1190 and 1104 cm^{-1}), $\text{Fe}(\text{Pc})\text{O}_2$ (1207 cm^{-1}), and $\text{Fe}(\text{salen})\text{O}_2$ (1106 cm^{-1}). The first two compounds form two isomeric dioxygen adducts whose O_2 stretching frequencies are ~ 1190 (isomer I) and $\sim 1105\text{ cm}^{-1}$ (isomer II). Isotope scrambling experiments ($^{16}\text{O}_2 + ^{16}\text{O}^{18}\text{O} + ^{18}\text{O}_2$) were carried out to elucidate the mode of coordination of dioxygen in these adducts. Neither isomer showed splitting of the $^{16}\text{O}^{18}\text{O}$ stretching band under the experimental conditions employed. Normal coordinate calculations predict that splitting should occur if dioxygen coordinates to the metal in the end-on fashion with a FeOO angle larger than 130° . We propose that isomer I possesses end-on geometry with the FeOO angle smaller than 130° whereas isomer II assumes symmetric side-on geometry. These structures are consistent with the observed relative intensities of the O_2 stretching bands, the proposed electronic ground states, and general spectra-structure relationships in a series of "base-free" dioxygen adducts of iron(II) chelates.

Recently, the matrix cocondensation technique has been used extensively to synthesize a number of novel and unstable compounds.¹ In this technique, the metal atom¹ or metal halide vapor² produced at high temperature is reacted with a ligand such as CO and O_2 diluted in inert gas and the reaction products are frozen immediately on a cold window (~ 15 K) for spectroscopic measurements. Vibrational spectra thus obtained provide valuable information about the structure and bonding of unstable or transient cocondensation products. We have already employed this technique for IR investigations of $\text{Co}(\text{TPP})\text{O}_2$ (TPP, tetraphenylporphyrinato anion),³ $\text{Co}(\text{acacen})\text{O}_2$ (acacen, N,N' -ethylenebis(acetylacetonate iminato) anion),⁴ $\text{Co}(\text{OEP})\text{O}_2$ (OEP, octaethylporphyrinato anion),⁵ and $\text{Co}(\text{J-en})\text{O}_2$ (J-en, N,N' -ethylenebis(2,2-diacetylmethylideneaminato) anion).⁶

In contrast to these Co(II) chelates, TPP complexes of Mn(II) and Fe(II) are air sensitive. In these cases, we have prepared $\text{Mn}(\text{TPP})\text{O}_2$ ⁷ and $\text{Fe}(\text{TPP})\text{O}_2$ ⁸ by preheating air-stable $\text{Mn}(\text{TPP})(\text{py})$ (py, pyridine) and $\text{Fe}(\text{TPP})(\text{pip})_2$ (pip, piperidine), respectively, in the Knudsen cell of our matrix isolation system

and by reacting the resultant $\text{Mn}(\text{TPP})$ and $\text{Fe}(\text{TPP})$, respectively, with O_2 diluted in argon. The IR spectrum of $\text{Fe}(\text{TPP})\text{O}_2$ thus obtained⁸ was of particular interest since it was the first example of a dioxygen adduct of a "base-free" and "unprotected" iron(II) porphyrin.⁹ Furthermore, we have found that $\text{Fe}(\text{TPP})\text{O}_2$ exists in two isomeric forms which exhibit the $\nu(\text{O}_2)$ (ν , stretching) at 1195 and 1106 cm^{-1} in Ar matrices. In order to understand the nature of these isomers, we have extended our study to the Fe(II) chelates of OEP, Pc (phthalocyanate anion), and salen (N,N' -ethylenebis(salicylideneaminato) anion). In particular, we have studied their reactions with $^{16}\text{O}^{18}\text{O}$ to elucidate the mode of coordination of dioxygen to the iron(II) center in the absence of axial base ligands.

Experimental Section

Compounds. All the Fe(II) chelates studied were prepared by the literature methods: $\text{Fe}(\text{TPP})(\text{pip})_2$,¹⁰ $\text{Fe}(\text{OEP})(\text{py})_2$,¹¹ $\text{Fe}(\text{Pc})(\text{py})_2$,¹² and $\text{Fe}(\text{salen})(\text{py})$.¹³ The gases, Ar (99.9995%), $^{16}\text{O}_2$ (99.99%), and $^{18}\text{O}_2$ (99.88%), were purchased from Matheson and Monsanto Research. A mixture of $^{16}\text{O}_2$, $^{16}\text{O}^{18}\text{O}$, and $^{18}\text{O}_2$ was prepared by electrical discharge of an equimolar mixture of $^{16}\text{O}_2$ and $^{18}\text{O}_2$ and its mixing ratio determined by Raman spectroscopy.

(9) Formation of $\text{Fe}(\text{TPP})\text{O}_2$ was also suggested by the recent ^1H NMR study (see Latos-Grazynski, L.; Cheng, T.-J.; La Mar, G. N.; Balch, A. L. *J. Am. Chem. Soc.* **1982**, *104*, 5992).

(10) Epstein, L. M.; Straub, D. K.; Maricondi, C. *Inorg. Chem.* **1967**, *6*, 1720.

(11) Bonnett, R.; Dimsdale, M. J. *J. Chem. Soc., Perkin Trans. 1* **1972**, 2540.

(12) Lever, A. B. P. *Adv. Inorg. Chem. Radiochem.* **1965**, *7*, 27.

(13) Niswander, R. H.; Martell, A. E. *Inorg. Chem.* **1978**, *17*, 2341.

(1) Moskovits, M.; Ozin, G. A. "Cryochemistry"; Wiley: New York, 1976.

(2) Tevault, D.; Nakamoto, K. *Inorg. Chem.* **1976**, *15*, 1282. Tevault, D.; Strommen, D. P.; Nakamoto, K. *J. Am. Chem. Soc.* **1977**, *99*, 2997.

(3) Kozuka, M.; Nakamoto, K. *J. Am. Chem. Soc.* **1981**, *103*, 2162.

(4) Urban, M. W.; Nonaka, Y.; Nakamoto, K. *Inorg. Chem.* **1982**, *21*, 1046.

(5) Urban, M. W.; Nakamoto, K.; Kincaid, J. *Inorg. Chim. Acta* **1982**, *61*, 77.

(6) Nakamoto, K.; Nonaka, Y.; Ishiguro, T.; Urban, M. W.; Suzuki, M.; Kozuka, M.; Nishida, Y.; Kida, S. *J. Am. Chem. Soc.* **1982**, *104*, 3386.

(7) Urban, M. W.; Nakamoto, K.; Basolo, F. *Inorg. Chem.* **1982**, *21*, 3406.

(8) Nakamoto, K.; Watanabe, T.; Ama, T.; Urban, M. W. *J. Am. Chem. Soc.* **1982**, *104*, 3744.

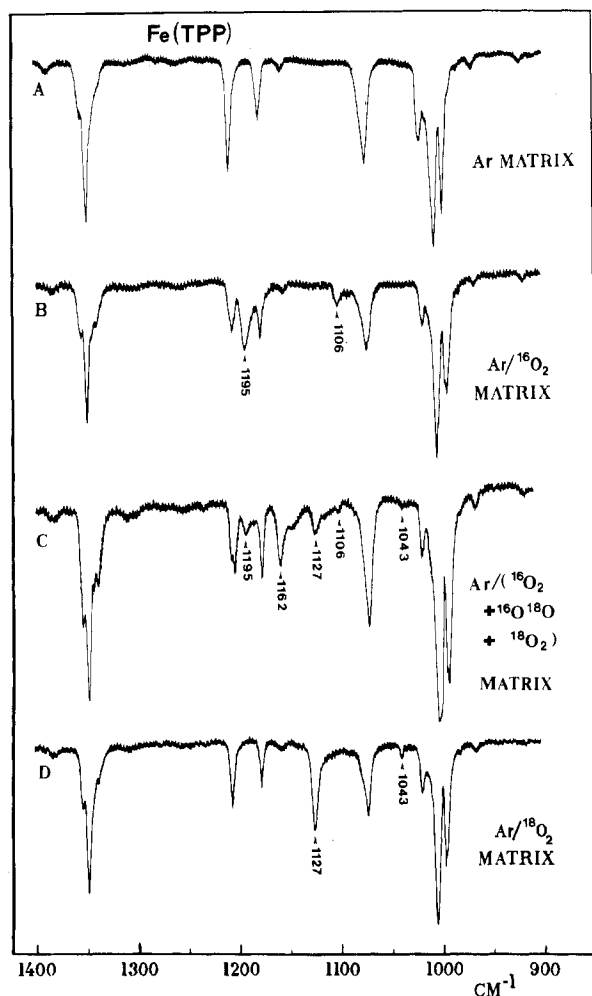


Figure 1. IR spectra of (A) Fe(TPP) in an Ar matrix, (B) Fe(TPP) cocondensed with 1:10 $^{16}\text{O}_2/\text{Ar}$, (C) Fe(TPP) cocondensed with 1:10 ($^{16}\text{O}_2 + ^{16}\text{O}^{18}\text{O} + ^{18}\text{O}_2$)/Ar, and (D) Fe(TPP) cocondensed with 1:10 $^{18}\text{O}_2/\text{Ar}$, all at ~ 15 K.

Spectral Measurements. The complex was placed in the Knudsen cell of our matrix-isolation system and heated under vacuum at 10^{-6} torr and 350–400 K for 4 h or longer until the vacuum gauge indicated complete dissociation of the axial base ligand from the complex. Heating was continued for another 2 h to ensure complete dissociation. The resulting base-free complex was vaporized from the Knudsen cell at 400–500 K and cocondensed with pure Ar or O_2 diluted in Ar on a CsI window which was cooled to ~ 15 K by a CTI Model 21 closed-cycle helium refrigerator. A thin film of Fe(TPP) was prepared by the same procedure in the absence of Ar.

IR spectra were measured on a Beckman Model 4260 infrared spectrophotometer with a $25\text{ cm}^{-1}/\text{in.}$ chart expansion and $5\text{ cm}^{-1}/\text{min}$ chart speed. Rotation-vibration bands of standard molecules and polystyrene film bands were used for frequency calibration.

Results and Discussion

Fe(TPP). Trace A of Figure 1 shows the IR spectrum of Fe(TPP) in an Ar matrix. When Fe(TPP) vapor was cocondensed with 1:10 $^{16}\text{O}_2/\text{Ar}$, two bands appeared at 1195 and 1106 cm^{-1} as is shown in trace B. These bands were shifted to 1127 and 1043 cm^{-1} , respectively, when Fe(TPP) was reacted with $^{18}\text{O}_2/\text{Ar}$ (1/10) (trace D). The observed isotopic shifts of these two bands (68 and 63 cm^{-1} , respectively) are in perfect agreement with that expected for the perturbed diatomic molecules. Furthermore, the 1:1 O_2/Fe stoichiometry of these O_2 adducts was confirmed by the observation that essentially the same spectra were obtained by changing the O_2/Ar dilution ratio in a wide range from pure O_2 to 1:1000 O_2/Ar .

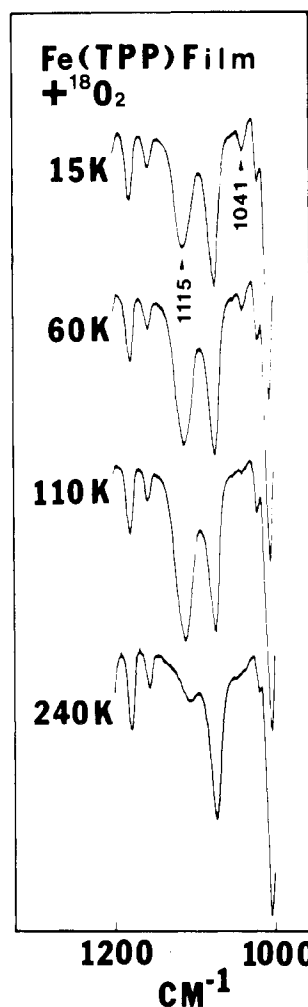


Figure 2. IR spectra of a thin film of Fe(TPP) reacted with $^{18}\text{O}_2$ at various temperatures.

The appearance of two $\nu(\text{O}_2)$ for Fe(TPP) O_2 is somewhat intriguing. The weaker band at 1106 cm^{-1} is not due to Fe-(TPP)(pip) O_2 since exactly the same spectrum was obtained when Fe(TPP)(py) $_2$ was used as the starting complex. The possibility of Fermi resonance with the first overtone of the $\nu(\text{Fe}-\text{O})^{14}$ or a porphyrin mode 15 is remote since both $^{16}\text{O}_2$ and $^{18}\text{O}_2$ adducts exhibit the same number of bands without any shifts of the TPP vibrations. The matrix site effect does not seem to be responsible since the intensity ratio of the two bands remains unchanged in a variety of matrix environments. In fact, Figure 2 shows that a thin film of Fe(TPP) reacted with $^{18}\text{O}_2$ exhibits a spectrum similar to that shown in Figure 1D. If this film is warmed, the band at 1115 cm^{-1} gains intensity at the expense of the band at 1041 cm^{-1} . Although the latter disappears at ~ 110 K, recoiling to ~ 15 K recovers its original intensity. These observations suggest that there are two isomers of Fe(TPP) O_2 and that isomer I is stable up to ~ 200 K (at which temperature it starts to decompose) whereas isomer II is converted to isomer I by raising the temperature to ~ 100 K. Furthermore, the molar intensity ratio of the $\nu(\text{O}_2)$ bands of these two isomers can be estimated from the spectra shown in Figure 2 since the isomer I \rightleftharpoons isomer II conversion involves the 1:1 stoichiometry. It was found that the $\nu(\text{O}_2)$ of isomer I is about 6.5 times stronger than that of isomer II.

Fe(OEP). Figure 3A shows the IR spectrum of Fe(OEP) in an Ar matrix. As expected, this spectrum is very similar to those of Ni(OEP) and Co(OEP) in Ar matrices for which complete IR

(14) Alben, J. O. In "The Porphyrins"; Dolphin, D., Ed.; Academic Press: New York, 1978; Physical Chemistry, Part A, p 334.

(15) Tsubaki, M.; Yu, N.-T. *Proc. Natl. Acad. Sci. U.S.A.* **1981**, *78*, 3581.

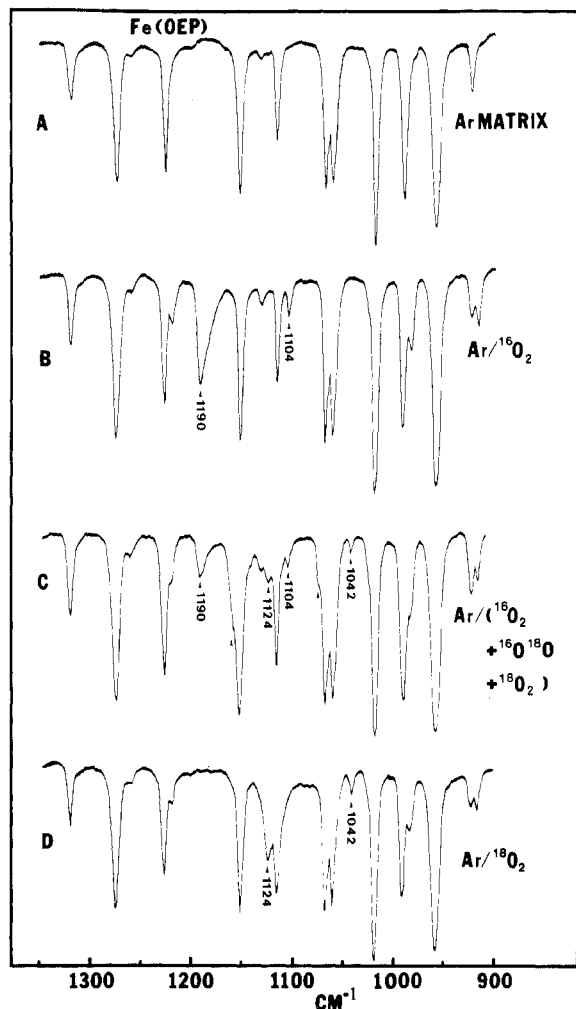


Figure 3. IR spectra of (A) Fe(OEP) in an Ar matrix, (B) Fe(OEP) cocondensed with 1:10 $^{16}\text{O}_2$ /Ar, (C) Fe(OEP) cocondensed with 1:10 ($^{16}\text{O}_2 + ^{16}\text{O}^{18}\text{O} + ^{18}\text{O}_2$)/Ar, and (D) Fe(OEP) cocondensed with 1:10 $^{18}\text{O}_2$ /Ar, all at ~ 15 K.

band assignments have been proposed on the basis of d_4 and ^{15}N substitutions.¹⁶ When Fe(OEP) vapor was cocondensed with 1:10 $^{16}\text{O}_2$ /Ar, two new bands were observed at 1190 and 1104 cm^{-1} as shown in trace B. These bands were shifted to 1124 and 1042 cm^{-1} , respectively, by $^{16}\text{O}_2$ - $^{18}\text{O}_2$ substitution (trace D). Again, the observed shifts of these bands (66 and 62 cm^{-1} , respectively) are very close to those expected for perturbed diatomic molecules (68 and 63 cm^{-1} , respectively). Based on the similarity of $\nu(\text{O}_2)$, we assign the 1190- and 1104- cm^{-1} bands to the $\nu(^{16}\text{O}_2)$ of isomers I and II of Fe(OEP) O_2 , respectively.

Previously, we observed that the OEP vibrations of Mn(OEP) at 1217, 980, and 911 cm^{-1} split into two bands when it forms Mn(OEP) O_2 .¹⁷ These splittings have been attributed to the lowering of the porphyrin core symmetry from D_{4h} to C_{2v} or lower. Figure 3 shows that the bands at 1227, 991, and 923 cm^{-1} of Fe(OEP) also split into two bands upon oxygenation. This observation suggests that symmetry lowering similar to that of Mn(OEP) O_2 occurs in either one or both isomers of Fe(OEP) O_2 . A warm-up experiment was also carried out for a thin film of Fe(OEP) O_2 . In this case, the isomer I band at 1174 cm^{-1} grew at the expense of the isomer II band at 1101 cm^{-1} as the temperature was raised, and the latter disappeared completely at ~ 100 K. Similar to the case of Fe(TPP) O_2 , the $\nu(\text{O}_2)$ band of the former was found to be about 6.7 times stronger than that of the latter.

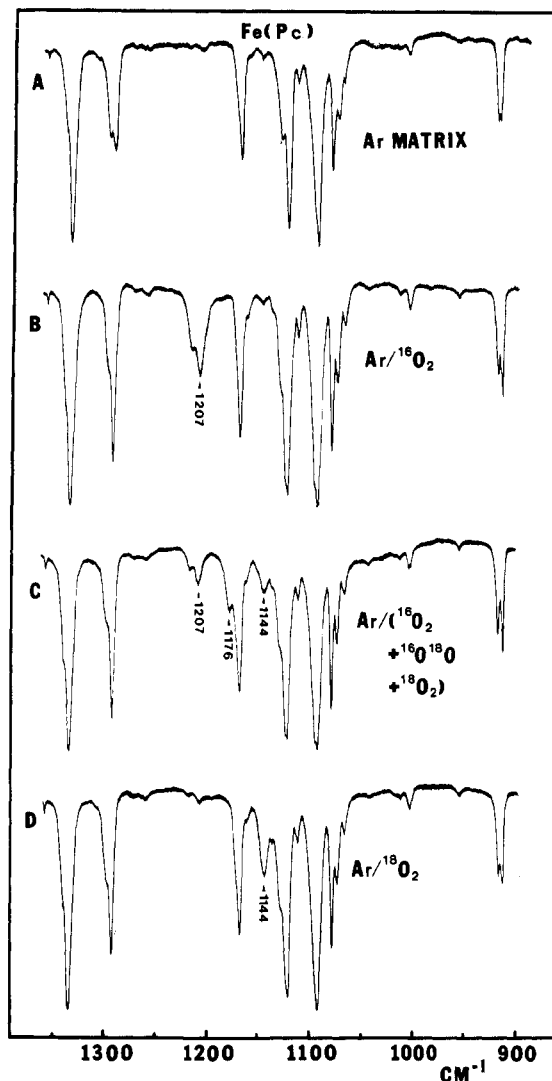


Figure 4. IR spectra of (A) Fe(Pc) in an Ar matrix, (B) Fe(Pc) cocondensed with 1:10 $^{16}\text{O}_2$ /Ar, (C) Fe(Pc) cocondensed with 1:10 ($^{16}\text{O}_2 + ^{16}\text{O}^{18}\text{O} + ^{18}\text{O}_2$)/Ar, and (D) Fe(Pc) cocondensed with 1:10 $^{18}\text{O}_2$ /Ar, all at ~ 15 K.

Fe(Pc). Figure 4A shows the IR spectrum of Fe(Pc) in an Ar matrix. This spectrum is similar to that of Mn(Pc) obtained in an Ar matrix¹⁷ and indicates that Fe(Pc) thus obtained is close to the α -form.¹⁸ As is seen in Figure 4B, a new band appears at 1207 cm^{-1} when Fe(Pc) is cocondensed with $^{16}\text{O}_2$ diluted in 1:10 Ar/ O_2 . This band can be assigned to the $\nu(^{16}\text{O}_2)$ of Fe(Pc) O_2 since it is shifted to 1144 cm^{-1} by $^{16}\text{O}_2$ - $^{18}\text{O}_2$ substitution (trace D). The shoulder band at 1218 cm^{-1} of trace B is assigned to a weak Pc mode since it also appears in traces A and D. Again we have confirmed the 1:1 O_2 /Fe stoichiometry of Fe(Pc) O_2 via dilution experiments. Only one $\nu(\text{O}_2)$ band which corresponds to isomer I of Fe(TPP) O_2 or Fe(OEP) O_2 was observed for Fe(Pc) O_2 . If a second isomer did exist, it would have shown $\nu(^{16}\text{O}_2)$ and $\nu(^{18}\text{O}_2)$ bands near 1105 and 1042 cm^{-1} , respectively.

Fe(salen). Figure 5A shows the IR spectrum of Fe(salen) in an Ar matrix. As is seen in trace B, a new band appears at 1106 cm^{-1} when Fe(salen) is codeposited with $^{16}\text{O}_2$ diluted in 1:10 Ar/ O_2 . This band is shifted to 1043 cm^{-1} by $^{16}\text{O}_2$ - $^{18}\text{O}_2$ substitution (trace D). These bands are assigned to $\nu(^{16}\text{O}_2)$ and $\nu(^{18}\text{O}_2)$, respectively, of Fe(salen) O_2 whose stoichiometry has been confirmed by dilution experiments. In contrast to Fe(Pc) O_2 , Fe(salen) O_2 shows only the $\nu(\text{O}_2)$ corresponding to isomer II of Fe(TPP) O_2 or Fe(OEP) O_2 .

(16) Kincaid, J. R.; Urban, M. W.; Watanabe, T.; Nakamoto, K. *J. Phys. Chem.* **1983**, *87*, 3096.

(17) Watanabe, T.; Ama, T.; Nakamoto, K. *Inorg. Chem.* **1983**, *22*, 2470.

(18) Stymne, B.; Sauvage, F. X.; Wettermark, G. *Spectrochim. Acta, Part A* **1979**, *35*, 1195. **1980**, *36*, 397.

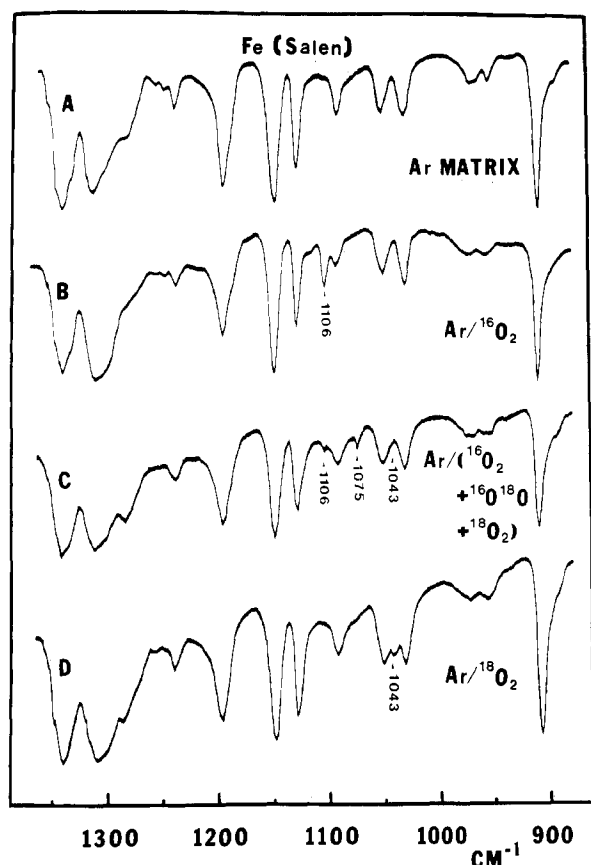
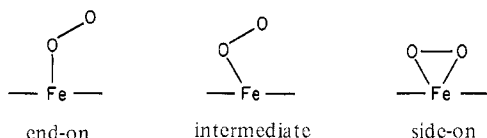


Figure 5. IR spectra of (A) Fe(salen) in an Ar matrix, (B) Fe(salen) cocondensed with 1:10 $^{16}\text{O}_2/\text{Ar}$, (C) Fe(salen) cocondensed with 1:10 ($^{16}\text{O}_2 + ^{16}\text{O}^{18}\text{O} + ^{18}\text{O}_2$)/Ar, and (D) Fe(salen) cocondensed with 1:10 $^{18}\text{O}_2/\text{Ar}$, all at ~ 15 K.

Mode of Dioxygen Coordination. The dioxygen molecule may take an end-on, side-on, or intermediate structure. So far, end-on



coordination has been confirmed by X-ray analyses of the dioxygen adducts of a picket-fence porphyrin (133° , 129°),¹⁹ hemoglobin (156°),²⁰ myoglobin (116°),²¹ and erythrocyrin (149°).²² (The number in the parentheses indicates the FeOO angle.) On the other hand, the intermediate structure with an acute FeOO angle and a slanted Fe-O bond has been proposed for Aplysia oxy-myoglobin on the basis of its polarized single-crystal electronic absorption spectrum²³ and for oxyferroporphyrin complexes on the basis of semiempirical MO calculations assuming a variety of coordination geometries for dioxygen.²⁴ Thus far, side-on coordination has been proposed only for the simple dioxygen adduct, FeO_2 , produced in an Ar matrix.²⁵

The isotope scrambling technique has been used widely to distinguish between end-on and side-on coordination of dioxygen and other homopolar diatomic ligands.¹ This is based on the premise that the side-on adduct having equivalent oxygen atoms

exhibits one $\nu(^{16}\text{O}^{18}\text{O})$ while the end-on adduct having non-equivalent oxygens exhibits two $\nu(^{16}\text{O}^{18}\text{O})$ bands (namely, $\nu(\text{Fe}-^{16}\text{O}^{18}\text{O})$ and $\nu(\text{Fe}-^{18}\text{O}^{16}\text{O})$) when an iron porphyrin is reacted with $^{16}\text{O}^{18}\text{O}$ produced by isotope scrambling. Previously, we³ have concluded that the dioxygen in "base-free" $\text{Co}(\text{TPP})\text{O}_2$ is end-on since $\text{Co}(\text{TPP})(^{16}\text{O}^{18}\text{O})$ exhibits two $\nu(^{16}\text{O}^{18}\text{O})$ bands at 1252 and 1241 cm^{-1} in an Ar matrix. Duff et al.²⁶ also confirmed the end-on coordination of dioxygen in oxyhemoglobin via the observation of two $\nu(\text{Fe}-\text{O})$ bands at 567 and 540 cm^{-1} in the resonance Raman spectrum of $^{16}\text{O}^{18}\text{O}$ hemoglobin.

In the present study, we have carried out matrix cocondensation reactions of Fe(TPP), Fe(OEP), Fe(Pc), and Fe(salen) with isotopically scrambled dioxygen ($^{16}\text{O}_2:^{16}\text{O}^{18}\text{O}:^{18}\text{O}_2 = 1:2:1$) diluted in Ar. Figure 1C shows that five $\nu(\text{O}_2)$ bands appear at 1195, 1162, 1127, 1106, and 1043 cm^{-1} when Fe(TPP) is cocondensed with the above isotopic mixture of dioxygen. All these bands except for the strong band at 1162 cm^{-1} have already been assigned in the preceding section. The 1162-cm^{-1} band must be assigned to the $\nu(^{16}\text{O}^{18}\text{O})$ of isomer I since its frequency is close to the average of $\nu(^{16}\text{O}_2)$ (1195 cm^{-1}) and $\nu(^{18}\text{O}_2)$ (1127 cm^{-1}). The corresponding $\nu(^{16}\text{O}^{18}\text{O})$ of isomer II is probably hidden under the strong Fe(TPP) band at 1076 cm^{-1} . In the case of Fe(OEP) O_2 , the $\nu(^{16}\text{O}^{18}\text{O})$ bands of isomers I and II are expected to appear near 1157 and 1073 cm^{-1} , respectively. Unfortunately, both are almost completely hidden under the strong Fe(OEP) bands (Figure 3C). Fe(Pc) O_2 exhibits the $\nu(\text{O}_2)$ of isomer I only. As is seen in Figure 4C, its $\nu(^{16}\text{O}^{18}\text{O})$ band appears as a shoulder at 1176 cm^{-1} and does not show any discernible splitting. Finally, the $\nu(^{16}\text{O}^{18}\text{O})$ band of Fe(salen) O_2 at 1075 cm^{-1} clearly indicates the absence of splitting (Figure 5C). Thus, no discernible splittings of the $\nu(^{16}\text{O}^{18}\text{O})$ bands were observed for all the dioxygen adducts studied above.

The average full width at half-height of the $\nu(\text{O}_2)$ of an Fe-(porphyrin) O_2 in an Ar matrix is $\sim 6\text{ cm}^{-1}$. Assuming the Lorentzian-shape band, we can show via computer simulation that the separation of two $\nu(^{16}\text{O}^{18}\text{O})$ bands of equal intensity cannot be detected unless their peak maxima are separated by more than 3.0 cm^{-1} . In the following section, we will show that splitting of the $\nu(^{16}\text{O}^{18}\text{O})$ band is expected to be less than 3.0 cm^{-1} for the asymmetric end-on structure having an acute FeOO angle (smaller than 130°). Thus, it is not possible to distinguish between the symmetric side-on structure (splitting is zero) and the asymmetric end-on structure with an acute FeOO angle (splitting is less than 3.0 cm^{-1}) in our experiments.

Normal Coordinate Calculations. In order to study the dependence of the $\nu(^{16}\text{O}^{18}\text{O})$ splitting on the FeOO angle, we have carried out normal coordinate calculations on the simple triatomic Fe-O-O model. First, we assumed the Fe-O and O-O distances to be 1.75 and 1.16 \AA , respectively, based on the results of X-ray analysis of the dioxygen adduct of a "base-bound" picket-fence porphyrin.¹⁹ Secondly, we employed three force constants, $K(\text{O}_2)$, $K(\text{FeO})$, and $H(\text{FeOO})$, the last being fixed at 0.2 mdyn/\AA .²⁷ Thirdly, the observed $\nu(^{16}\text{O}_2)$ and $\nu(\text{Fe}-^{16}\text{O})$ were taken to be 1195 [$\nu(^{16}\text{O}_2)$ of isomer I of $\text{Fe}(\text{TPP})\text{O}_2$] and $\sim 380\text{ cm}^{-1}$, respectively. Since we were not able to observe the latter in Ar matrices, we estimated it based on the observation that the $\nu(\text{Co}-\text{O})$ of $\text{Co}(\text{TPP})\text{O}_2$ is at 345 cm^{-1} (resonance Raman spectrum) in an Ar matrix³ and that the $\nu(\text{Fe}-\text{O})$ is $\sim 30\text{ cm}^{-1}$ higher than the $\nu(\text{Co}-\text{O})$ in metalloporphyrins (~ 570 vs. $\sim 540\text{ cm}^{-1}$).¹⁵ Thus far, the Fe-O-O bending band has not been observed. We, therefore, assumed that any calculations which estimate its frequency below 250 cm^{-1} are reasonable. We have calculated the best set of force constants to fit these frequencies for a given Fe-O-O angle (α). Figure 6 plots $K(\text{O}_2)$ and $K(\text{FeO})$ thus obtained as a function of α . Trace b shows the result obtained for a set in which the $\nu(\text{Fe}-\text{O})$ was assumed to be 380 cm^{-1} . Since this value is only approximate, we carried out similar calculations assuming the

(19) Jameson, G. B.; Robinson, W. T.; Gagne, R. R.; Reed, C. A.; Collman, J. P. *Inorg. Chem.* **1978**, *17*, 850.

(20) Shaanan, B. *Nature (London)* **1982**, *296*, 683.

(21) Phillips, S. E. V. *J. Mol. Biol.* **1980**, *142*, 531.

(22) Steigemann, W.; Weber, E. *J. Mol. Biol.* **1979**, *127*, 309.

(23) Makinen, M. W.; Churg, A. K.; Glick, H. A. *Proc. Natl. Acad. Sci. U.S.A.* **1978**, *75*, 2291.

(24) Kirchner, R. F.; Loew, G. H. *J. Am. Chem. Soc.* **1977**, *99*, 4639.

(25) Chang, S.; Blyholder, G.; Fernandez, J. *Inorg. Chem.* **1981**, *20*, 2813.

(26) Duff, L. L.; Appelman, E. H.; Shriver, D. F.; Klotz, I. M. *Biochem. Biophys. Res. Commun.* **1979**, *90*, 1098.

(27) Duff-Weddell, L. L. Ph.D. Thesis, Northwestern University, Evanston, IL, 1981.

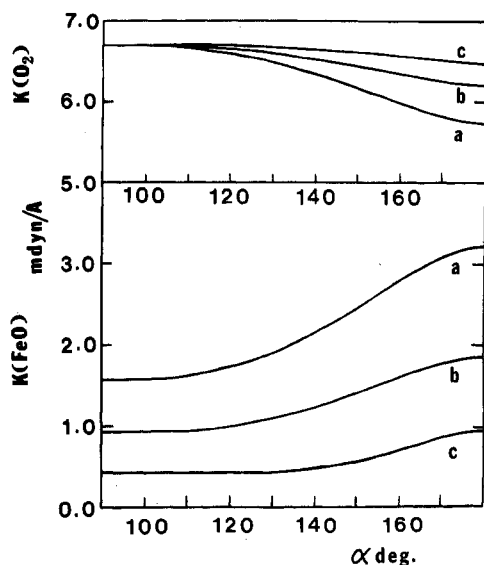


Figure 6. Plots of $K(\text{O}_2)$ and $K(\text{FeO})$ as a function of the FeOO angle (α). Traces a, b, and c denote the results obtained by assuming that the $\nu(\text{Fe-O})$ is at 480, 380, and 280 cm^{-1} , respectively.

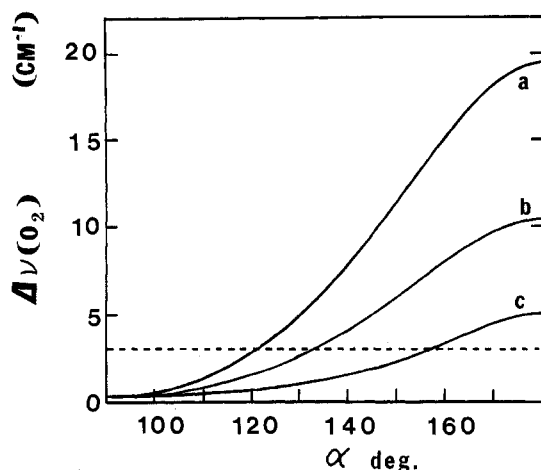


Figure 7. Plots of $\Delta\nu(\text{O}_2)$ vs. FeOO angle (α). Traces a, b, and c represent the results obtained by assuming that the $\nu(\text{Fe-O})$ is at 480, 380, and 280 cm^{-1} , respectively.

$\nu(\text{Fe-O})$ to be 480 (trace a) and 280 cm^{-1} (trace c). It is seen in all three cases that $K(\text{O}_2)$ and $K(\text{FeO})$ are almost invariant in the range of $\alpha = 90$ to 120° , and change rapidly as α increases from 120 to 170° .

Next, we calculated the magnitude of the isotope splitting, $\Delta\nu(\text{O}_2) = \nu(\text{Fe-}^{16}\text{O}^{18}\text{O}) - \nu(\text{Fe-}^{18}\text{O}^{16}\text{O})$, using the set of force constants obtained for each α . Figure 7 is a plot of $\Delta\nu(\text{O}_2)$ as a function of α . As stated in the previous section, the splitting of the $\nu(^{16}\text{O}^{18}\text{O})$ band is observable under our experimental conditions if the two bands are separated by more than 3 cm^{-1} . In Figure 7, we have drawn the horizontal dotted line to indicate this limit. It shows that under condition b, which is most probable, the splitting due to the end-on coordination cannot be observed unless α is greater than $\sim 130^\circ$. Since $\Delta\nu(\text{O}_2)$ depends markedly upon the value of the $\nu(\text{Fe-O})$, the maximum value of α which gives the observable splitting also depends upon the assumed $\nu(\text{Fe-O})$ value. Although trace c estimates this angle to be $\sim 160^\circ$, this condition is highly unlikely as discussed in the preceding section. On the other hand, trace a estimates this angle to be 120° which is smaller than that for trace b. Thus, we conclude that the distinction of end-on and side-on coordination cannot be made on the basis of the $\nu(^{16}\text{O}^{18}\text{O})$ splitting if the FeOO angle is smaller than 130° (acute angle).

Similar calculations were also made to estimate the splitting of the $\nu(\text{Fe-O})$ mode. Figure 8 plots the isotope splitting, $\Delta\nu$

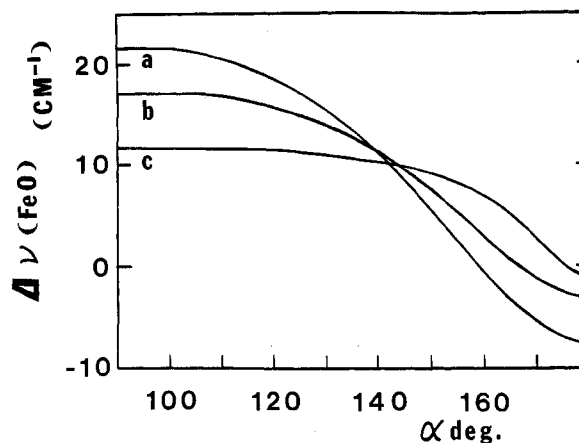


Figure 8. Plots of $\Delta\nu(\text{Fe-O})$ vs. FeOO angle (α). Traces a, b, and c represent the results obtained by assuming the $\nu(\text{Fe-O})$ to be at 480, 380, and 280 cm^{-1} , respectively.

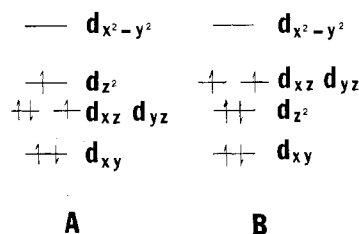


Figure 9. Two possible electron configurations for Fe(porphyrin).

$(\text{Fe-O}) = \nu(\text{Fe-}^{16}\text{O}^{18}\text{O}) - \nu(\text{Fe-}^{18}\text{O}^{16}\text{O})$ as a function of α . All three traces show that $\Delta\nu(\text{Fe-O})$ is fairly constant in the range of $\alpha = 90$ to 120° and decreases rapidly as α becomes larger than 120° . Since $\Delta\nu(\text{Fe-O})$ is large (22–12 cm^{-1} in the range of $\alpha = 90$ to 130°), the end-on geometry is easily recognized by isotope scrambling experiments.²⁶ Furthermore, the side-on structure is expected to show two $\nu(\text{Fe-O})$ (symmetric and antisymmetric) modes which are substantially separated and exhibit no splitting for the $^{16}\text{O}^{18}\text{O}$ species. Unfortunately, these criteria are not applicable to our studies since it was not possible to prepare matrices thick enough to observe them.

Structure Isomers of Fe(porphyrin) O_2 . As discussed above, it is rather difficult to distinguish between the end-on structure with an acute FeOO angle and the symmetric side-on structure by the isotope scrambling technique. Since no other techniques are currently available for the structure determination of matrix-isolated species, we speculate on the most probable structures of the two isomers of Fe(porphyrin) O_2 based on the following information:

(1) **IR Intensity of the $\nu(\text{O}_2)$ Band.** As stated earlier, the $\nu(\text{O}_2)$ band of isomer I is about six times stronger than that of isomer II. This result readily rules out the possibility of rotational isomers involving the relative orientation of the Fe-O-O plane with respect to the FeN_4 or FeN_2O_2 core. Since the symmetry rule predicts that the $\nu(\text{O}_2)$ band of the end-on dioxygen should be much more intense than that of the side-on dioxygen, it is reasonable to conclude that isomer I takes the end-on structure while isomer II takes the side-on structure. As discussed in the previous section, however, the former should have an acute FeOO angle possibly with a slanted Fe-O bond.^{23,24}

(2) **Electronic Ground State of Fe(porphyrin).** Two possible electronic ground states have been proposed for the four-coordinate, square-planar Fe(TPP) molecule having an intermediate spin state ($S = 1$). Zerner et al.²⁸ suggests the $(d_{xy})^2(d_{xz}, d_{yz})^3(d_{z^2})^1$ configuration (Figure 9A) whereas Collman et al.²⁹ proposes the $(d_{xy})^2(d_{z^2})^2(d_{xz}, d_{yz})^2$ configuration (Figure 9B). The former tends

(28) Zerner, M.; Gouterman, M.; Kobayashi, H. *Theor. Chim. Acta* **1966**, 6, 363.

(29) Collman, J. P.; Hoard, J. L.; Kim, N.; Lang, G.; Reed, C. A. *J. Am. Chem. Soc.* **1975**, 97, 2676.

TABLE I: Effect of In-Plane Ligand on O₂ Stretching Frequency (cm⁻¹)

Co(TPP)O ₂	1278 (end-on) ^a
Co(OEP)O ₂	1275 (end-on) ^b
Fe(Pc)O ₂	1207 (I)
Fe(TPP)O ₂	1195 (I), 1106 (II)
Fe(OEP)O ₂	1190 (I), 1104 (II)
Fe(salen)O ₂	1106 (II)
Mn(Pc)O ₂	992 (side-on) ^c
Mn(TPP)O ₂	983 (side-on) ^d
Mn(OEP)O ₂	991 (side-on) ^c

^a Reference 3. ^b Reference 5. ^c Reference 17. ^d Reference 7.

to favor the end-on structure since one unpaired electron occupies the d_{z²} orbital³⁰ whereas the latter tends to take the symmetric side-on structure since two unpaired electrons occupy the d_{xz} and d_{yz} orbitals.³¹ Since the energy gap between these two states is expected to be small, the matrix cocondensation reaction may produce a mixture of end-on and side-on species.

(30) Dedieu, A.; Rohmer, M.-M.; Veillard, A. *J. Am. Chem. Soc.* **1976**, *98*, 5789.

(31) Hanson, L. K.; Hoffman, B. M. *J. Am. Chem. Soc.* **1980**, *102*, 4602.

(3) *Structure-Spectra Relationship.* As is shown in Table I, Co(porphyrin)O₂ ($\nu(\text{O}_2) \sim 1275 \text{ cm}^{-1}$) is of the end-on type whereas Mn(porphyrin)O₂ ($\nu(\text{O}_2) \sim 990 \text{ cm}^{-1}$) is of the side-on type. This seems to suggest that, in a series of M(porphyrin)O₂ type compounds, the adduct having a higher $\nu(\text{O}_2)$ tends to take the end-on structure while the adduct having a lower $\nu(\text{O}_2)$ tends to take the side-on structure. In the case of Fe(porphyrin), the $\nu(\text{O}_2)$ of isomer I is closer to that of Co(porphyrin)O₂ whereas that of isomer II is closer to that of Mn(porphyrin)O₂. This suggests that isomer I is of the end-on variety while isomer II is of the side-on type. Finally, such a structure-spectra relationship predicts that the dioxygen in Fe(Pc)O₂ is end-on whereas that in Fe(salen)O₂ is side-on. Namely, the mode of dioxygen coordination depends upon the size of the π -conjugated chelate ring around the Fe atom.

Acknowledgment. This work was supported by the National Science Foundation (Grants CHE-8205522 and PCM-8114676). We thank Professor D. P. Strommen of Carthage College for his valuable comments.

Registry No. Fe(TPP)O₂ (isomer I), 67887-55-2; Fe(TPP)O₂ (isomer II), 88083-22-1; Fe(OEP)O₂ (isomer I), 74455-49-5; Fe(OEP)O₂ (isomer II), 88083-23-2; Fe(Pc)O₂, 88105-32-2; Fe(salen)O₂, 88083-24-3.

Infrared Spectrum of the C₂F₅ Free Radical Trapped in Solid Argon in Discharge Sampling Experiments

Marilyn E. Jacox

Molecular Spectroscopy Division, National Bureau of Standards, Washington, D.C. 20234

(Received: May 25, 1983)

When the products of the reaction between F atoms formed in a microwave discharge and C₂F₄ are frozen in a large excess of argon at 14 K, prominent absorptions of C₂F₃ and C₂F₆ appear in the infrared spectrum of the solid deposit. All of the absorptions above 400 cm⁻¹ previously attributed to C₂F₃ except that near 1040 cm⁻¹ have been confirmed. Very little fragmentation of C₂F₃ occurs under the conditions of these experiments. The most prominent absorptions of C₂F₃ are also present in the infrared spectrum of the quenched products of the excitation of an Ar:C₂F₆ sample in a low-power microwave discharge, but rupture of the C=C bond predominates in the corresponding study of discharged Ar:C₂F₄ samples. The vibrational assignment of the C₂F₃ spectrum and the processes which account for the observed product distribution in the F + C₂F₄ experiments are discussed.

Introduction

The C₂F₃ free radical may be expected to play an important role in the chemistry of high-energy systems in which fluorocarbons are present. These systems are exemplified by fluorocarbon discharges, which have provided the basis for the recent development of new techniques for microcircuit etching.¹ Although Smolinsky and co-workers^{2,3} did not detect C₂F₃ in mass spectrometric studies of the products of radio-frequency discharges through C₂F₄ and C₂F₆ in a flow system, it would have been difficult to have distinguished the C₂F₃ cracking pattern from the composite pattern of the other products. Infrared or ultraviolet spectroscopic detection of C₂F₃ would offer the advantage of specificity, with the added bonus of remote sensing. High detection sensitivity has been achieved with pumped dye lasers in the visible and near ultraviolet and various high-resolution laser-based techniques in the infrared. No electronic transitions of C₂F₃ have been observed. However, the infrared spectrum of C₂F₃, produced by the pyrolysis of C₂F₃I and trapped in solid argon, has recently been reported.⁴ The stabilization of C₂F₃ in other systems would

test this identification and would facilitate the development of techniques for the study of the high-resolution gas-phase infrared spectrum of this free radical.

The reaction of F atoms with C₂F₄, the subject of several previous investigations, provides a suitable alternate source of C₂F₃. In studies of the reaction of thermalized fluorine-18 atoms with various fluoroethylenes, Rowland and co-workers⁵ found that the F + C₂F₄ reaction occurs less readily than does the reaction with the hydrogen-containing fluoroethylenes. This reaction is exothermic with respect to the formation of CF₂ + CF₃, and decomposition into these products was observed. In a later mass spectrometric study of this reaction system, Butkovskaya and co-workers⁶ reported evidence for collisional stabilization of C₂F₃.

A series of experiments in this laboratory has been concerned with the spectroscopic characterization of the products of the reaction of F atoms produced in a discharge with various small molecules, frozen in a large excess of argon. In the first such study,^{7a} using NF₃ and CF₄ as F-atom sources, reaction with

(1) J. W. Coburn and E. Kay, *IBM J. Res. Dev.*, **23**, 33 (1979).

(2) M. J. Vasile and G. Smolinsky, *J. Phys. Chem.*, **81**, 2605 (1977).

(3) E. A. Truesdale and G. Smolinsky, *J. Appl. Phys.*, **50**, 6594 (1979).

(4) R. Butler and A. Snelson, *J. Fluorine Chem.*, **15**, 89 (1980).

(5) T. Smail, R. S. Iyer, and F. S. Rowland, *J. Am. Chem. Soc.*, **94**, 1041 (1972).

(6) N. I. Butkovskaya, M. N. Larichev, I. O. Leipunskii, I. I. Morozov, and V. L. Tal'roze, *Dokl. Akad. Nauk SSSR*, **240**, 366 (1978); *Dokl. Phys. Chem.*, **240**, 442 (1978).